NUMERICAL HYDRODYNAMICS FROM GAS-KINETIC THEORY

Kun Xu

Submitted in partial fulfillment of the

requirements for the degree

of Doctor of Philosophy

in the Graduate School of Arts and Sciences

COLUMBIA UNIVERSITY

1993

ABSTRACT

NUMERICAL HYDRODYNAMICS FROM GAS-KINETIC THEORY

Kun Xu

A new high-resolution numerical hydrodynamic scheme is developed from considerations of gas-kinetic theory. This Boltzmann-type scheme uses the particle distribution function, and follows its evolution to evaluate the numerical fluxes. The intrinsic multidimensional property in the evolution stage of the gas distribution function distinguishes it from any other high order upwind scheme. From the approximate Boltzmann equation, the Navier-Stokes equations can be derived, and this new numerical method uses this advantage to approximate the solutions of the Navier-Stokes equations, where the advection and dissipation effects are coupled in the time-dependent gas distribution function. Several well-defined numerical test cases are presented in one and two dimensions, and it is shown that the resolution in the numerical results is competitive with those of any of the current high-resolution schemes without special treatment of the discontinuities; for strong rarefaction waves, our scheme gives better results. In this thesis, we try to separate clearly numerical and physical effects, and we also give a concise explanation of the necessity of including numerical viscosities implicitly or explicitly in high-resolution Godunov-type and central difference schemes, even for the Navier-Stokes equations. The main part of this thesis will be published in two papers ([28] and [45]) in the Journal of Computational Physics.

CONTENTS

LIST OF FIGURES

Acknowledgement

It is my pleasure to offer my gratitude and thanks to my advisor Kevin H. Prendergast, who introduced me to the problem, guided and encouraged me throughout the course of this work, and to Prof. Ami Harten, who kindly gave me his comments and suggestions, and offered his unforgettable help in the past years. I am indebted to Prof. Jacqueline van Gorkom, Edward Spiegel, C.K. Chu, James Applegate, Norman Baker and Edward Shara for their kindly teaching and encouragment during the whole period of my graduate study at Columbia. I would also like to thank all my predecessors and friends in the CFD community, Prof. P. L. Roe, B. van Leer, H.C. Yee, C.W. Shu, S. Jin, J.G. Liu, Y.H. Qian and V. Modi; their stimulating discussion and sharp questioning made me understand more broadly and deeply the work I am doing. I also owe special thanks to all of my teachers, colleagues and fellow students at Columbia for making me feel welcome and helping me develop my scientific and technical skills.

I thank Prof. T.D.Lee for sponsoring the CUSPEA (China & United States Physics Examination & Application) program on which I had the chance to begin my education at Columbia.

I also deeply thank my parents and teachers in China for their caring, encouraging and educating.

Last but not the least, special thanks go to my wife Jie Shen for sharing all the good and bad times with me. Without her love , support and help, this thesis would never be finished.

Introduction

This work presents a new numerical scheme, starting from an approximation to the Boltzmann equation, to solve the Navier-Stokes and Euler equations. The most successful Boltzmann model equation is perhaps the Bhatnagar-Gross-Krook (BGK or Krook) model [2], which describes how the real gas distribution function f relaxes to an equilibrium distribution function g on a time scale τ determined by the collisions between the molecules. The new numerical scheme in this thesis is based on the integral solution of the BGK model, along with conservation constraints for the mass, momentum and energy densities during collision. Combining this last condition with the formal solution of the BGK equation leads to a set of coupled integral equations for the parameters of the time-dependent evolution of the real gas distribution function, from which the numerical fluxes are evaluated. It is well-known that the Euler and Navier-Stokes equations can be derived from the solution of the BGK model, by using the Chapman-Enskog expansion. The Euler equations are the limit of the Navier-Stokes equations when the physical viscosity approaches zero, or equivalently, the collision time τ is goes to zero. The numerical approach to the BGK model in this thesis solves (not surprisingly) the Navier-Stokes equations without separating the advection and dissipation terms, as well as the Euler equations.

Another important aspect in our new numerical scheme is that it couples the spatial and temporal accuracy in the evolution of flow by following individual particle's trajectories in space and time. This property also makes the scheme more "multidimensional" in the evolution stage than other current semi-multidimensional schemes, although the advantages of multidimensionality in our scheme has not yet been totally developed. For most TVD (Total Variation Diminishing) and ENO (Essentially Nonoscillatory) schemes [37], Runge-Kutta methods are usually used to

achieve high-order accuracy in time by solving the so-called semi-discrete equations. We do not need these (expensive) intermediate steps.

In chapter 1 we give an introduction to early Boltzmann-type schemes and review some numerical methods. A detailed analysis of the physical reasons for their limitations as Euler or Navier-Stokes solvers are discussed.

Starting from the gas kinetic theory in chapter 2, we develop our new scheme based on the BGK model. Chapter 2 will emphasize the numerical Navier-Stokes solutions, and also demonstrate the methods' accuracy by showing its behavior on some well-known test cases. Theoretically, the transition from the Navier-Stokes equations to the Euler equation is made by reducing the physical viscosity to zero. In practice, since discontinuities emerge inside the gas flow, the viscosity needed in the real simulation have to balance both the physical reliability and the numerical stability requirements in order to achieve high resolution results, where the finite cell size plays an important role.

In chapter 3, we first make a smooth transition from the Navier-Stokes scheme in chapter 2 to the Euler scheme by starting from a new physical interpretation for the necessity of numerical viscosity. Following that, the numerical method for the Euler equations is tested on a number of well-defined cases, and the results show clearly that this scheme is in every way comparable or superior to other schemes found in the current literature.

In the conclusion, we will demonstrate the multidimensional character of our current scheme and offer some comments about future work.

Chapter One: Early Boltzmann-Type Schemes

1.1 Relations between Hydrodynamics and the Gas-Kinetic Theory

There are two ways to describe the gas flow; the first one is based on macroscopic quantities, such as mass, momentum and energy densities, and the physical law governing these quantities can be the Euler, Navier-Stokes or higher order approximate equations. Another type of description comes from microscopic considerations, *e.g.* the gas kinetic theory, and the fundamental quantity is the particle distribution function $f(x_i, u_i, t)$, which gives the number densities of molecules in the six-dimensional phase space $(x_i, u_i) = (x, y, z, u, v, w)$.

The governing equation for the time-evolution of the gas distribution function f is the Boltzmann equation, if binary collisions are dominant. There are many ways to derive the Boltzmann equation — one of them is the direct derivation from a particle collisional model, as Boltzmann did. The most physical derivation is from general theorems of statistical mechanics, *i.e.* the Liouville Equation; the derivation constitutes the so-called **BBGKY**-hierarchy (from the names of Bogoliubov, Born, Green, Kirkwood and Yvon) (Cercignani [5]) , where collisions of all orders (double and triple, *etc.*) are considered in successive approximations.

For sufficiently rarefied gases, two body collisions are most important and to this order of approximation, the general accepted Boltzmann Equation is

$$f_t + u_i f_{x_i} + a_i f_{u_i} = Q(f, f), \tag{1.1}$$

where the f is the one-particle probability distribution, x_i, u_i and a_i are particle location, velocity and force terms acting on the particle respectively, and $Q(f, f)$

is the integral collision operator. From the physical constraints of conservation of mass, momentum and energy during collisions, the following condition is satisfied:

$$\int \Psi_\alpha Q(f,f) d\Xi = 0, \tag{1.2}$$

where $d\Xi = du_1 du_2 du_3 d\xi$ and $\psi_\alpha = \{1, u_i, \frac{1}{2}({u_i}^2 + \xi^2)\}$ with ξ being twice the energy in internal degrees of freedom. (The detailed explanation for ξ is left to section(2.2).) From the Boltzmann equation, the Navier-Stokes and Euler equations can be obtained from Eq.(1.1) by using the so-called Chapman-Enskog expansions (Chapman-Cowling [6]).

Before we get to the relation between the Boltzmann equation and the hydrodynamic equations, let us first introduce the macroscopic description of the gas flow. Hydrodynamic Equations for the conservation laws can be described as equations for the density, momentum and energy densities,

$$\rho(x_j,t) \quad ; \quad \rho(x_j,t)U_i(x_j,t) \quad ; \quad \frac{\rho U^2}{2} + \rho\epsilon_i(x_j,t), \tag{1.3}$$

where ϵ_i is the internal energy density, and U_i is the velocity of the hydrodynamic flow.

The conservation laws for these functions can be written in the following form (Landau and Lifshitz [21]):

Equation of continuity

$$\frac{\partial \rho}{\partial t} + \frac{\partial \rho U_j}{\partial x_j} = 0, \tag{1.4}$$

Equation of momentum

$$\frac{\partial \rho U_i}{\partial t} + \frac{\partial \rho U_i U_j}{\partial x_j} = -\frac{\partial p}{\partial x_i} - \frac{\partial \pi_{ij}}{\partial x_j} + \rho F_i \tag{1.5}$$

Equation of energy

$$\frac{\partial}{\partial t}[\frac{\rho U^2}{2} + \epsilon_i] + \frac{\partial}{\partial x_i}[U_i(\frac{\rho U^2}{2} + \rho\epsilon_i + p) + \pi_{ij}U_j + S_i] = \rho F_i U_i. \tag{1.6}$$

The closure of the equations (1.4)-(1.6) is based on two hypotheses, which are 1). The existence of a local thermodynamic equilibrium. This allows us to use the second law of thermodynamics for the gas, which hold for quasi-static processes

$$Tds = d\epsilon_i + pd(\frac{1}{\rho}) \quad ; \quad \mathcal{S}(x_j,t) = \rho(x_j,t)s(x_j,t) \tag{1.7}$$

and the empirical equation of state,

$$p = p(\rho,T) \quad ; \quad \epsilon_i = \epsilon(\rho,T), \tag{1.8}$$

where s and T are entropy density and temperature.

2). The existence of two linear dissipative relations: Newton's formula for the force of internal friction, and Fick's formula for the vector of thermal flux S_i. Newton's formula is used in generalized form for the viscous stress tensor π_{ij}. These formula have the form

$$\pi_{ij} = -\eta[\frac{\partial U_i}{\partial x_j} + \frac{\partial U_j}{\partial x_i} - \frac{2}{3}\delta_{ij}\frac{\partial U_k}{\partial x_k}] - \zeta\delta_{ij}\frac{\partial U_k}{\partial x_k};$$

$$S_i = -\kappa\frac{\partial T}{\partial x_i}. \tag{1.9}$$

The first of these relations expresses the viscous stress tensor in terms of the derivatives of the velocity, and the second links the thermal flux vector with the gradient of the temperature. Within the framework of phenomenological theory the coefficients of viscosity η, ζ, and the coefficient of thermal conductivity κ are measured experimentally as functions of ρ and T. As a result, we have a closed set of equations for the "hydrodynamic" variables of ρ, U_i and T.

For a gas, the equations of fluid dynamics can be compared with the Boltzmann equation for the distribution function f, which are linked *via* the expressions

$$\rho = \int f d\Xi \quad ; \quad \rho U = \int f u d\Xi \quad ; \quad \frac{1}{2}\rho U^2 + \epsilon_i = \int f\frac{1}{2}(u^2+\xi^2)d\Xi. \tag{1.10}$$

The transition from the Boltzmann equation to the relevant gas-dynamic equations is possible under the additional conditions

$$Kn = l/L << 1 \quad , \quad \frac{1}{Re} = \frac{\nu}{UL} \sim \frac{Kn}{M} << 1. \tag{1.11}$$

Here the Kn is the Knudsen number, l is the mean free path of atoms, L is the characteristic scale of the hydrodynamic flow, Re is the Reynolds number, M is the Mach number, U is the characteristic velocity of the hydrodynamic flow, and finally ν is the kinematic viscosity. From the Boltzmann equation the quantities ν and κ can be derived as functions of the basic quantities describing the molecules. In Appendix A, we give a detailed derivation of the Navier-Stokes equations from an approximate model of the Boltzmann equation and find expressions for the parameters ν , ζ and κ.

For time-dependent equilibrium or near-equilibrium flow, kinetic theory has been directly applied to the Euler or slightly compressible Navier-Stokes equations. The calculation of the solutions from the Boltzmann equation are limited to some very simple situations, as for Couette flow, using perturbation methods. Some of the widely used methods for solving nonequilibrium gas flow problems are due to the numerical approaches of the gas-kinetic equations.

1.2 The Beam Scheme and High-order Extensions

In an important and influential paper, Harten, Lax and van Leer[13] draw a distinction between two numerical approaches to the solution of the Euler equations, namely, Godunov and Boltzmann-type schemes. Broadly speaking, a Godunov scheme relies on solving a Riemann problem; Boltzmann schemes embody a distribution function of particle velocities, where the characteristics are trajectories of individual particles of the gas instead of sound waves and streamlines. The prototypical Godunov scheme is, of course, Godunov's scheme, which is first-order, and

therefore of comparatively low accuracy. There exists a rich literature of high-order schemes incorporating some of the devices in Godunov's scheme, particularly the use of solutions of the Riemann problem, either exact or approximate: these include many of the TVD and ENO schemes [15]. In this section, we will introduce an early-type Boltzmann scheme and show numerical results for some well-defined test cases.

One of the early numerical hydrodynamical schemes based on considerations of gas-kinetic theory is the beam scheme (Sanders and Prendergast [34]). Before we explain what the beam scheme is, let's look at the following problem. One of the well-known problems in almost all elementary gas-kinetic text books is the following: Suppose there is a box containing a gas in an equilibrium state, with number density n and temperature T, and outside this box is a vacuum. Now suppose we suddenly open a small hole at one side of the box; what are the particle fluxes across this small hole? The standard procedure for doing this problem is: first, construct an equilibrium Maxwellian distribution function for this classical ideal gas corresponding to the specific particle density and temperature, which is

$$g = Ae^{(-\lambda(u_i-U_i)^2+\xi^2)}, \tag{1.12}$$

where $\lambda = 1/kT$, k is the Boltzmann constant and T is the temperature, U_i is the macroscopic velocity which is equal to zero for this problem, u_i and ξ are individual particle velocity and internal velocities, and A is the normalization constant. Second, find mass, momentum and energy fluxes across the small hole; these are given by the integration of the Maxwellian over the velocity space (assuming the fluxes are in the x direction),

$$\begin{pmatrix} F_\rho \\ F_{P_i} \\ F_\epsilon \end{pmatrix} = \int_{u_1>0} u_1 \begin{pmatrix} 1 \\ u_i \\ \frac{1}{2}({u_k}^2+\xi^2) \end{pmatrix} g d\Xi, \tag{1.13}$$

where $d\Xi = \xi^{K-1} d\xi du_i$, and K, the number of internal degrees of freedom of the gas particles, is related to the ratio of specific heat γ by $K = -3 + 2/(\gamma - 1)$. For a monatomic gas ($K = 0$), the mass flux is $\frac{1}{4} n\bar{v}$, where the $\bar{v}$ is the average absolute velocity of the particles, with $\bar{v} = (8kT/m\pi)^{1/2}$, where m is the molecular mass and T is the temperature. This problem is also called the gas effusion problem.

The direct transition from the above problem to a numerical code for the hydrodynamical equations is the beam scheme, and the basic idea of the beam scheme is the following: *(For the purpose of simplicity, we illustrate the beam scheme in the one-dimensional case. For two and three dimensions, similar equations can be found easily. This property of easy extrapolation of kinetic schemes to higher dimensions is one of the distinguishable characteristics of Boltzmann-type schemes.)* In the one-dimensional case, the physical space is divided into cells (i refers to i_{th}cell); inside each cell the average physical quantities are given: mass ρ , momentum P and total energy ϵ, from which the Maxwellian distribution function (Eq.(1.12)) can be constructed by using the relation between the parameters of the particle distribution function and the macroscopic quantities,

$$\begin{pmatrix} \rho \\ P \\ \epsilon \end{pmatrix} = \begin{pmatrix} A\pi^{(K+1)/2}\lambda^{-(K+1)/2} \\ \rho U \\ \frac{1}{2}\rho(U^2 + \frac{K+1}{2\lambda}) \end{pmatrix}. \tag{1.14}$$

For convenience of numerical calculation, we usually use ρ, λ, U instead of A, λ, U to describe the Maxwellian distribution (see Appendix B). By solving Eq.(1.14), all parameters in the Maxwellian g can be determined from macroscopic quantities:

$$\begin{pmatrix} \rho \\ U \\ \lambda \end{pmatrix} = \begin{pmatrix} \rho \\ P/\rho \\ (K+1)\rho/(4(\epsilon - \frac{1}{2}\rho U^2)) \end{pmatrix}. \tag{1.15}$$

Once we know the Maxwellian distribution function, as in the problem of gas effusion from the box, the mass, momentum and energy fluxes across the cell boundary can

be easily found from

$$\begin{pmatrix} F_\rho \\ F_P \\ F_\epsilon \end{pmatrix}_{i+1/2}^{BEAM} = \int_{u>0} u \begin{pmatrix} 1 \\ u \\ \frac{1}{2}(u^2+\xi^2) \end{pmatrix} g_i d\Xi + \int_{u<0} u \begin{pmatrix} 1 \\ u \\ \frac{1}{2}(u^2+\xi^2) \end{pmatrix} g_{i+1} d\Xi, \tag{1.16a}$$

where $i+1/2$ is the boundary between cells i and $i+1$, and g_i and g_{i+1} are the Maxwellians inside cells i and $i+1$ respectively. The implicit assumption in the above scheme for particle propagation is that there are NO collisions between the positive velocity particles at the boundary coming from the left cell and the negative velocity particles from the right cell. This assumption is the basic property of the beam scheme and is consistent with the intrinsic upwind method, where physical properties are directly included in the discretization of the flow equations.

In order to understand the beam scheme further and to make it easier to analyze in the next section, let's use a more specific numerical language to restate the beam scheme . Usually a numerical scheme is composed of two stages, the reconstruction and evolution stages. For the beam scheme, the reconstruction is the preparation of the initial Maxwellian inside each cell,

$$g_0(x) = \begin{cases} g_i, & x<0 \\ g_{i+1}, & x>0 \end{cases} \tag{1.16b}$$

where $x=0$ is assumed to be the boundary between cell i and $i+1$. In the evolution stage, the initial data are propagated according to the collisionless Boltzmann equation , which is

$$g_t + u g_x = 0, \tag{1.16c}$$

with the solution

$$g_{i+1/2} = g_0(x-ut)\,\big|_{x=0} = g_0(-ut) = \begin{cases} g_i, & u>0 \\ g_{i+1}, & u<0 \end{cases} \tag{1.16d}$$

where $i+1/2$ is the boundary between cell i and $i+1$, and the evolution time t is always larger than zero. If we put Eq.(1.16d) into the definitions of the fluxes, the fluxes for the beam scheme (Eq.(1.16a)) can be obtained.

The evaluation of the integral in Eq.(1.16a) is not hard, and is given in Appendix B. Knowing the fluxes, the amount of mass, momentum and energy transferred from one cell to another are equal to the integrals of the fluxes over the time step Δt. The CFL (Courant-Lewy-Friedrichs) stability condition for Δt has to be used in this explicit scheme; this requires, roughly speaking, the numerical information propagation speed to be greater than the physical signal propagation speed. The above procedure can be repeated to simulate the time evolution of the gas flow. This scheme is first order, and as is true for other first order schemes, the simulation results show the effect of strong diffusion. It will be shown in the next section that the numerical gas viscosity and heat conductivity in this scheme depend on the grid size Δx.

Before we give a detailed analysis of the beam scheme, let's first see some numerical examples using this scheme. In the following, the Sod, Lax-Harten and Woodward-Colella test cases are presented.

• Sod Shock Tube [39]: This test case is a one dimensional shock tube problem with two different initial constant states in the left and right parts of the tube — $\rho_l = 1, P_l = 0, \epsilon_l = 2.5$ and $\rho_r = 0.125, P_r = 0, \epsilon_r = 0.25$. This is a standard Riemann problem with a similarity solution. There are three waves; shock, contact discontinuity and rarefaction, emerging from the location of the initial discontinuity. The results from the beam scheme are shown in Fig(1.1a) for the density, velocity and pressure distributions, where the solid lines are the exact solutions. 200 points were used in this test.

• Lax-Harten Shock Tube ([22]): Similar to the Sod test case, the Lax-Harten test has initial conditions $\rho_l = 0.445, P_l = 0.311, \epsilon_l = 8.928$ and $\rho_r = 0.5, P_r = 0.0, \epsilon_r =$

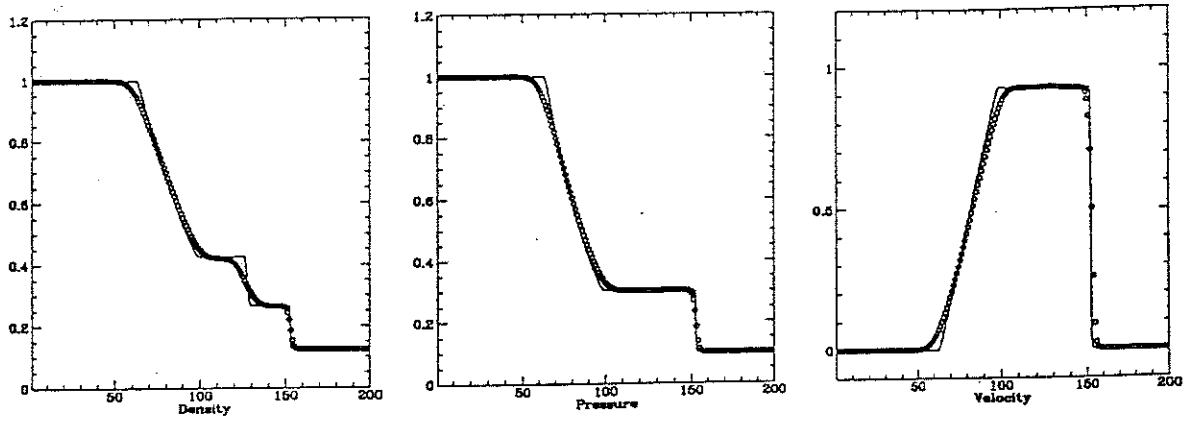

Figure 1.1a : Sod test case from 1st order beam scheme

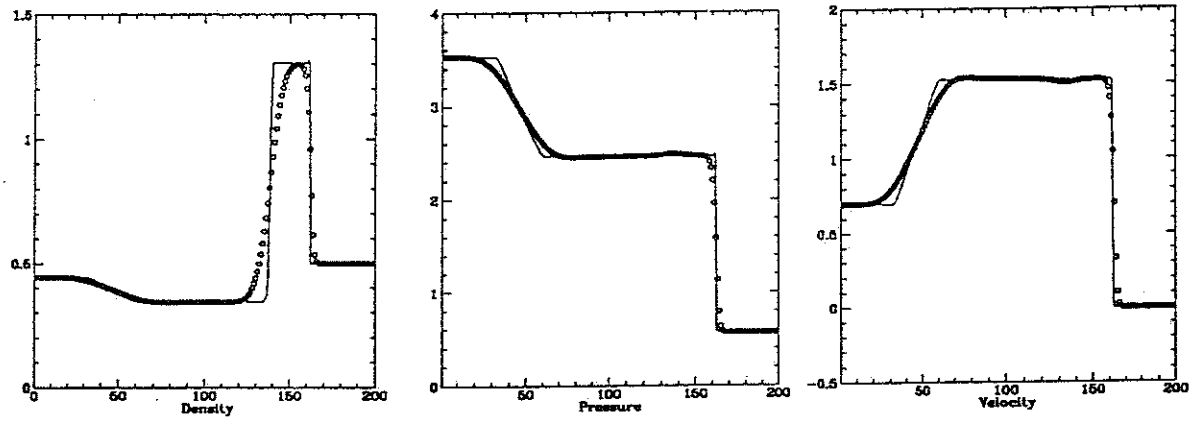

Figure 1.1b : Lax-Harten test case from 1st order beam scheme

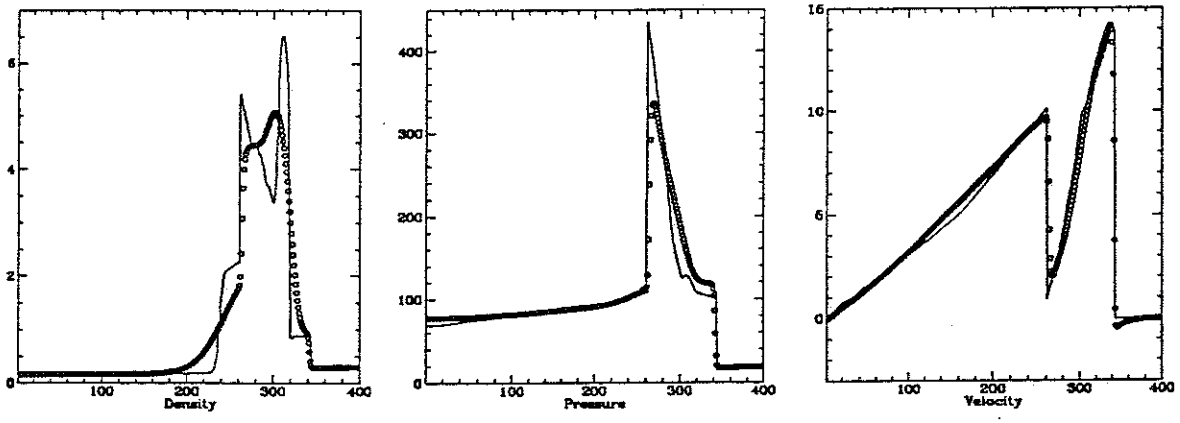

Figure 1.1c : Woodward-Colella test case from 1st order beam scheme

1.4275, which gives much stronger shock and contact discontinuity waves than the Sod test. The results are shown in Fig(1.1b), also using 200 points.

• Woodward-Colella Test Case: This test case is from a paper by Woodward and Colella [44]. The initial condition consists of three constant states, each of which is at rest, between reflecting walls separated by a distance of unity, with $\rho_l = 1.0, P_l = 0, \epsilon_l = 2500$ for $0 < x \leq 0.1$, $\rho_m = 1.0, P_m = 0.0, \epsilon_m = 0.025$ for $0.2 < x \leq 0.9$ and $\rho_r = 1.0, P_r = 0.0, \epsilon_r = 250$ for $0.9 < x \leq 1$. Two strong blast waves develop and collide, producing new contact discontinuities. This is a very difficult test case. The density, velocity and pressure profiles are shown in Fig(1.1c) for 400 points.

In all three test cases, we can see the diffusive character of the beam scheme, which is similar to that of all other first order schemes, such as Godunov and Lax-Friedrichs schemes. But, as we will analyze in the next section, the reason for the diffusivity in the beam scheme is different from any other (non-Boltzmann) type schemes.

The beam scheme was first used in an astronomical simulation in the 1970s. At that time, the evaluation of the error function was very expensive, so three delta functions were used to replace the Maxwellian distribution function. Due to this fact, Roe[31] and other authors (Harten *et al* [13]) regarded the Steger-Warming's [40] flux splitting method (which also has three characteristic waves derived from the Euler equations (Hirsch [16])) as a rediscovery of the beam scheme. Actually they are totally different: one comes from the collisionless Boltzmann equation and the other from the Euler equations (which should have an infinite number of collisions). Although their first order schemes give similar results, the second and higher order schemes differ considerably. The reason is that for any first order scheme, the artificial viscosity from the reconstruction stage is always dominant over the real physical one.

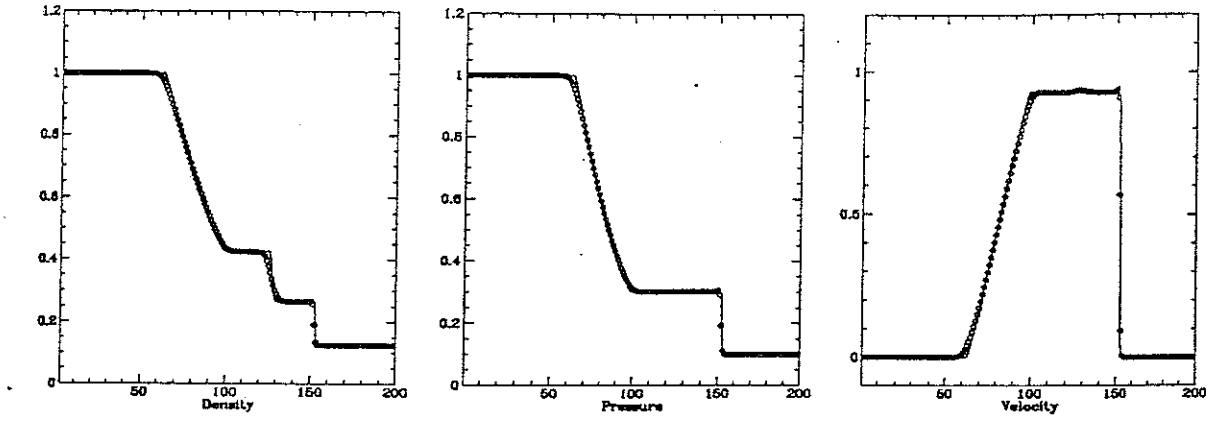

Figure 1.2a : Sod test case from 2nd order beam scheme

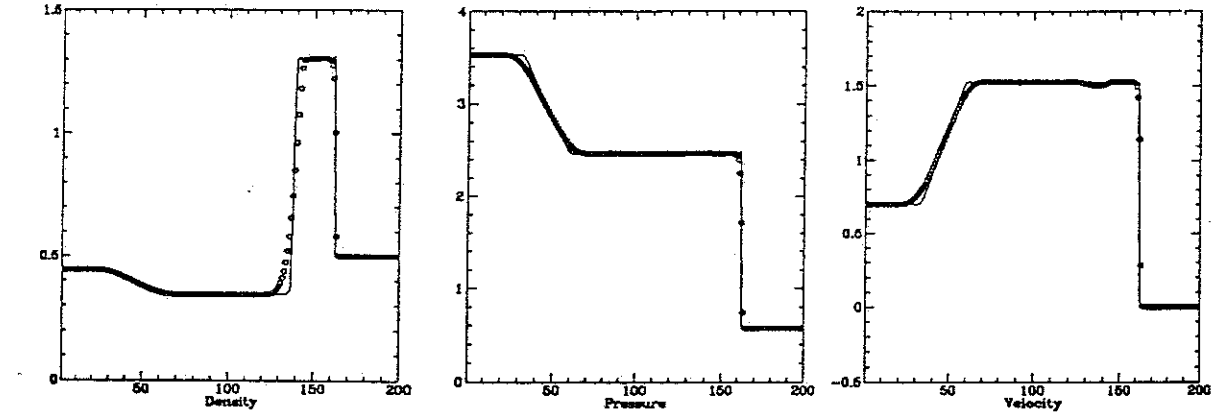

Figure 1.2b : Lax-Harten test case from 2nd order beam scheme

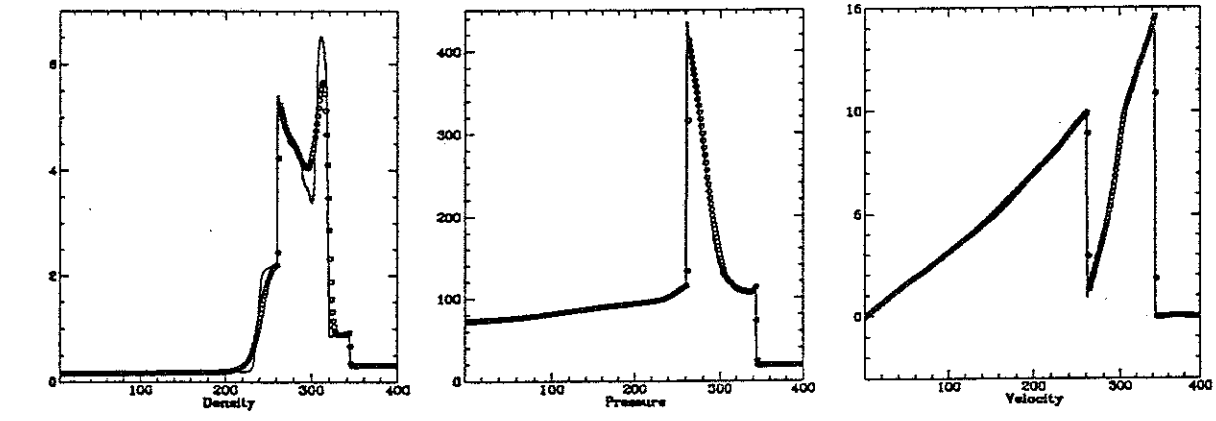

Figure 1.2c : Woodward-Colella test case from 2nd order beam scheme

Beginning in the 1980's, the idea of the beam scheme was re-invented, modified, or extended by many authors , such as Reitz[30] , Pullin[28], Deshpande[10] and Perthame[26]. Pullin was the first to use the complete error functions to get the numerical fluxes, and Perthame used some other simplified equilibrium state to replace the Maxwellians. As for high-order Godunov-type schemes, higher-order versions of the beam scheme have been constructed (by van Albada *et. al.* [42], Perthame [26] and Deshpande [10] *ect.*). Some of them use high-order interpolations for the mass, momentum and energy inside each cell to get two new values at a cell boundary, from which two new Maxwellians are constructed. Perthame has given a more detailed and generalized mathematical analysis of Boltzmann schemes in several papers (see references in [26]). In the following, we give an extension of the beam scheme to second order, the idea being similar to Perthame's second order schemes, but technically it is different. First, instead of Eq.(1.16b), we interpolate the initial gas distribution as

$$g_0(x) = \begin{cases} g_l(1 + a_l x), & x < 0 \\ g_r(1 + a_r x), & x > 0 \end{cases} \tag{1.18a}$$

where terms a_l and a_r are from the Taylor expansion of the Maxwellian distribution and their parameters can be found from the mass, momentum and energy expansions around the cell boundary. [In chapter 2, there is a detailed explanation of this, and the above equation corresponds to Eq.(2.42), the initial term in our new one dimensional scheme]. According to the collisionless Boltzmann equation, the distribution function at the cell boundary is

$$g_{i+1/2} = g_0(x - ut)\,\big|_{x=0} = \begin{cases} g_l(1 - a_l ut), & u > 0 \\ g_r(1 - a_r ut), & u < 0 \end{cases} \tag{1.18b}$$

where $i+1/2$ is the cell boundary between i and $i+1$. The final mass, momentum and energy transferred between cells are

$$\begin{pmatrix} F_\rho \\ F_P \\ F_\epsilon \end{pmatrix}_{i+1/2} = \int_0^T \int_{u>0} u \begin{pmatrix} 1 \\ u \\ \frac{1}{2}(u^2+\xi^2) \end{pmatrix} g_l(1-a_l u t) d\Xi dt + \int_0^T \int_{u<0} u \begin{pmatrix} 1 \\ u \\ \frac{1}{2}(u^2+\xi^2) \end{pmatrix} g_r(1-a_r u t) d\Xi dt, \qquad (1.18c)$$

where T is the time step. Fig(1.2a) — Fig(1.2c) are the simulation results from the second order beam scheme, where a simple slope-limiter is used for the interpolations of the macroscopic variables to prevent the values at a cell boundary from over or under shooting. Theoretically, third and even higher order beam scheme can be constructed along these lines, using TVD and ENO methods . But the real performance of the scheme will not only be determined by the high-order interpolations, but also by the governing equation in the evolution stage.

1.3 An Analysis of the Beam Scheme

As pointed out earlier, there are similarities between the beam scheme and the first order Godunov scheme, where two constant states are used at the beginning of each time step, the solution of the numerical fluxes across the cell boundary are constant inside each time step, and both of the numerical results are diffusive. But, due to their intrinsically different physical origins, the behavior of the Boltzmann-type schemes are much easier to understand physically.

In most current literature about Boltzmann schemes the beam scheme or other versions are regarded having the Euler equations as the limit when the time step Δt approaches zero. Actually they are different from the Euler solutions:

• The general procedure of deriving the Euler equations from the Boltzmann equation is based on the assumption that the local gas distribution remains in an equilibrium state, with a Maxwellian distribution. It is true in the beam scheme that

the gas distribution is initially Maxwellian inside each cell, but the real gas distribution function (*cf.* Eq.(1.16d)) which is used to evaluate the numerical fluxes across the cell boundary is actually not Maxwellian at all — it is composed of "two half-Maxwellians" defined for particle velocities $u > 0$ and $u < 0$. Inserting the "two half-Maxwellians" as the distribution function f into the Boltzmann equation or its approximate models, and integrating the equations for the three moments (in the 1-D case), cannot give the Euler equations, even in the limit of $t \to 0$, because the discontinuity at $u = 0$ in the distribution function will give heat conduction, viscosity and even higher moment terms. So, in order to make the numerical scheme be consistent with the Euler equations, the Maxwellian should be constructed at the cell boundary to evaluate fluxes. The direct use of a Maxwellian constructed from the interpolated macroscopic quantities at a cell boundary would definitely give oscillatory results in discontinuity regions. This is similar to the behavior of early central-difference schemes which had no artificial viscosities. In order to incorporate more physical reality into the beam scheme, two new schemes (TTT and PTT) are discussed in the next section.

• The transport of the numerical fluxes in the beam scheme is computed from the collisionless Boltzmann equation $g_t + ug_x = 0$ with the solution of $g = F(x - ut)$. This property is absolutely contradictory to the physical requirement for the validity of the Euler equations. The Euler equations need the moments of the right side of the collision term in the Boltzmann equation to go to zero, not the collision term *itself* to be zero. On the contrary, there need be many collisions to adjust the gas distribution to the equilibrium Maxwellian distribution locally and "instaneously". In order to incorporate physical collisions, a more physical Boltzmann model will be considered in this thesis.

• The Euler equations are the limit when the physical viscosity approaches zero, or equivalently, the collision time between particles goes to zero. In the beam

scheme , the collisions are included implicitly at the end of each time step in the preparation of the Maxwellian for the calculation of fluxes in the next time step , which effectively endows the gas with a mean collision time close to the CFL time, and that is much too long for the real gas flow. Actually, the molecules in a real gas suffer many collisions during a CFL time step, and these collisions insure that the molecules have a near-Maxwellian velocity distribution in the Navier-Stokes limit. Macrossan [23] show that the final viscosity and heat conductivity of the first order beam scheme depend on the grid size Δx, with

$$\eta = \sqrt{RT/2\pi}\rho\Delta x, \tag{1.18a}$$

and

$$\kappa = (\gamma + 1)C_v\sqrt{RT/8\pi}\rho\Delta x, \tag{1.18b}$$

where C_v is the specific heat at constant volume, and γ is specific heat ratio. If we go one step further, from Eq.(1.18), the relation between molecular mean free path l and grid size Δx can be derived, which is $l = \Delta x/2$, and it is totally artificial. These relations are independent of the time step Δt, so the beam scheme is NOT the limit of the Euler equations even at $\Delta t \to 0$.

For higher-order versions of the beam scheme the viscosity and heat conductivity coefficients will be different from the above values. But, without re-examining the physical origin of the method, any high-order interpolation for the mass, momentum and energy in each cell cannot help recover the physical particle collisions. Still, the collisionless Boltzmann equation is the root and is solved in the evolution stage for most Boltzmann-type schemes. This is different from Godunov-type scheme, where the Euler equations are used in the evolution stage, using a so-called Riemann solver. This is also the reason why the high-order Godunov schemes have a better numerical behavior than the high-order beam schemes. In other words, the intrinsic physical property in the beam scheme allows the particles in the high

temperature region freely to penetrate into the low temperature region without any collisions, and strongly to smear the temperature gradient in these regions. This effect is clearly observed in the regions of the contact discontinuity in the 1-D and slip lines in 2-D cases, and the smearing will not be much decreased by using high-order initial interpolations, especially for high dimensional problems.

1.4 Modification of the Beam Scheme

In order to include collisions in the beam scheme, one extreme case is to assume that the particles from the left and right sides of the cell boundary collide at the boundary, and from the mass, momentum and energy of the collision products, a new Maxwellian distribution function is constructed at this point, from which the numerical fluxes can be evaluated. This kind of scheme, with instantaneous collisions, will be called a TTT scheme (Totally Thermalized Transport), which can be written in mathematical format in two steps. For the first order TTT scheme, first, the collected mass, momentum and energy at the cell boundary $i+1/2$ from the initial distribution (Eq.(1.16d)) is,

$$\begin{pmatrix} \rho_{i+1/2} \\ P_{i+1/2} \\ \epsilon_{i+1/2} \end{pmatrix} = \int_{u>0} \begin{pmatrix} 1 \\ u \\ \frac{1}{2}(u^2+\xi^2) \end{pmatrix} g_i d\Xi + \int_{u<0} \begin{pmatrix} 1 \\ u \\ \frac{1}{2}(u^2+\xi^2) \end{pmatrix} g_{i+1} d\Xi. \quad (1.19)$$

Second, from $\rho_{i+1/2}, P_{i+1/2}$ and $\epsilon_{i+1/2}$, we construct a new Maxwellian $g_{i+1/2}$ (Eq.(1.12)), and then the numerical fluxes are obtained from $g_{i+1/2}$ as

$$\begin{pmatrix} F_\rho \\ F_P \\ F_\epsilon \end{pmatrix}^{TTT}_{i+1/2} = \int u \begin{pmatrix} 1 \\ u \\ \frac{1}{2}(u^2+\xi^2) \end{pmatrix} g_{i+1/2} d\Xi. \quad (1.20)$$

For the second order extension, we can put Eq.(1.18b) instead of Eq.(1.16d) into Eq.(1.19) to get $\rho_{i+1/2}, P_{i+1/2}$ and $\epsilon_{i+1/2}$. Then, the same equation (1.20) is used to get fluxes and integrate them over time to get the total mass, momentum and energy

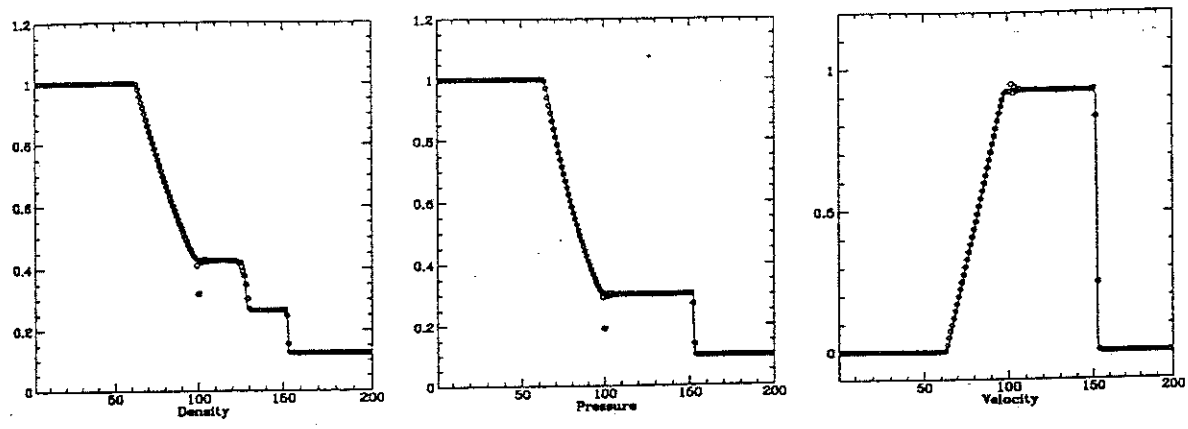

Figure 1.3a : Sod test case from 2nd order TTT scheme

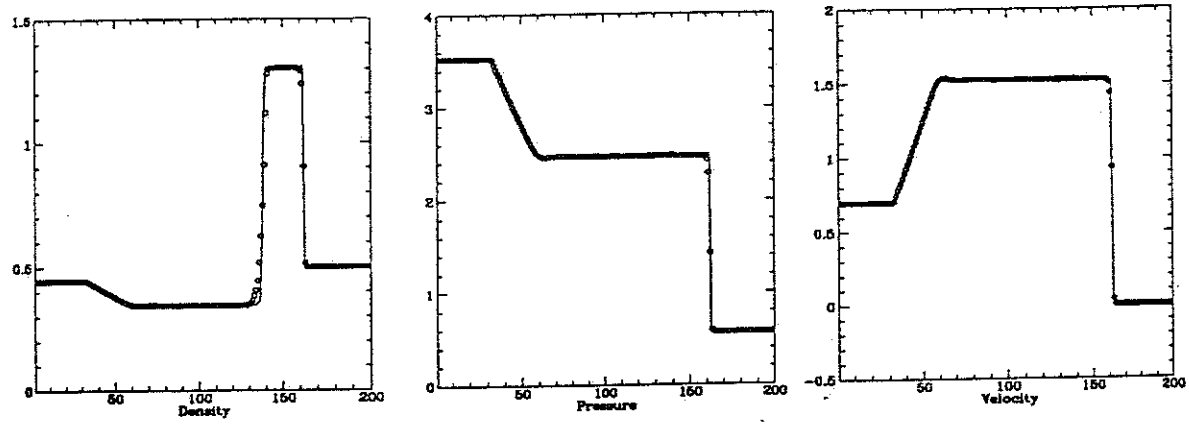

Figure 1.3b : Lax-Harten test case from 2nd order TTT scheme

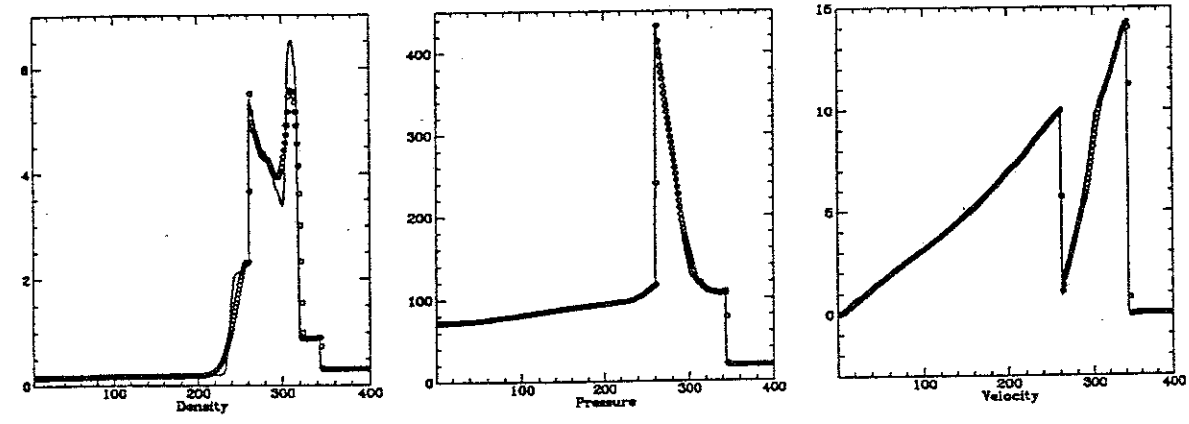

Figure 1.3c : Woodward-Colella test case from 2nd order TTT scheme

transport in a time step. Some numerical examples from the above second-order TTT scheme are shown in Fig(1.3a) — Fig(1.3c) .

As shown in the figures, the TTT scheme gives a much lower dissipation than the beam scheme in the numerical results, but with errors in the corner of the rarefaction wave, especially in the Sod test case. The reason for generating errors in the TTT scheme is that the particles from the left and right hand cells cannot collide totally at the cell boundary. Actually during the whole passage of particles moving toward to the cell boundary, they undergo many collisions and would not collide instantaneously just at the cell boundary; in fact, many of them can even penetrate some distance into the other cell without any collisions. The real physical situation requires a relaxation process for the particle collisions.

One of the more reasonable schemes should be the combination of TTT with the beam scheme, which includes both collision and free transport conceptually, and the percentage of the two can be determined from numerical experience, or calculated from some detailed physical model. This combined scheme can be called PTT scheme (Partial Thermalized Transport), and the final numerical fluxes at the cell boundary are

$$\begin{pmatrix} F_\rho \\ F_P \\ F_\epsilon \end{pmatrix}^{PTT}_{i+1/2} = \hat{\eta} \begin{pmatrix} F_\rho \\ F_P \\ F_\epsilon \end{pmatrix}^{BEAM}_{i+1/2} + (1-\hat{\eta}) \begin{pmatrix} F_\rho \\ F_P \\ F_\epsilon \end{pmatrix}^{TTT}_{i+1/2}, \tag{1.21}$$

where $\hat{\eta}$ is the percentage for the beam scheme fluxes. Fig(1.4a) — Fig(1.4c) show the simulation results from a second order PTT schemes, with $\hat{\eta} = 20\%$. From these figures, we see that the errors have been reduced.

The TTT and PTT schemes arise purely from "physical intuition", and the use of $\hat{\eta}$ is similar to the adoption of the artificical viscosity in the early central difference schemes. From the history of the development of central-difference schemes, we can believe that more work is needed to determine the parameter $\hat{\eta}$ as a function of local

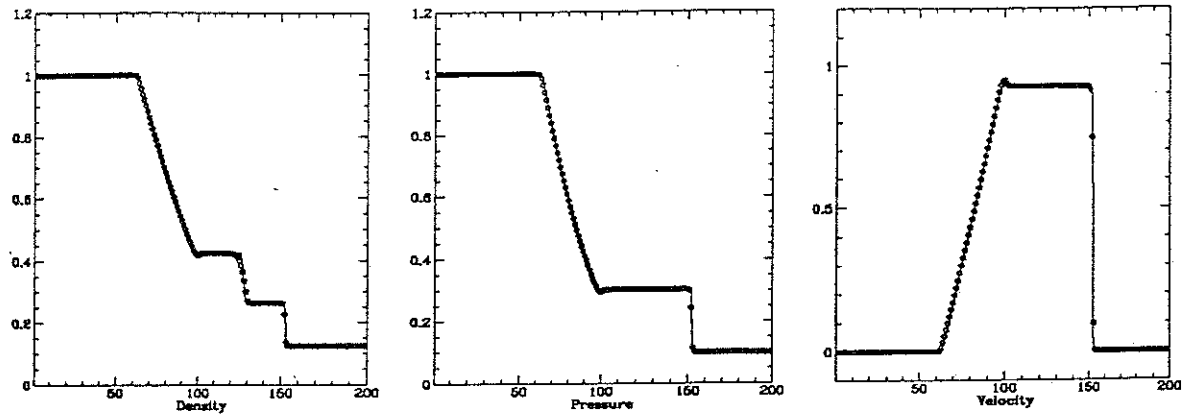

Figure 1.4a : Sod test case from 2nd order PTT scheme

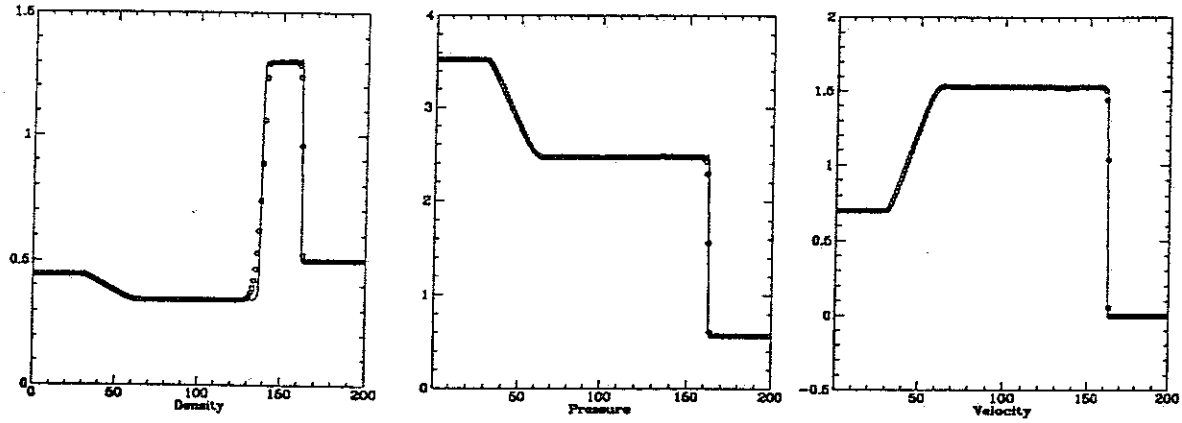

Figure 1.4b : Lax-Harten test case from 2nd order PTT scheme

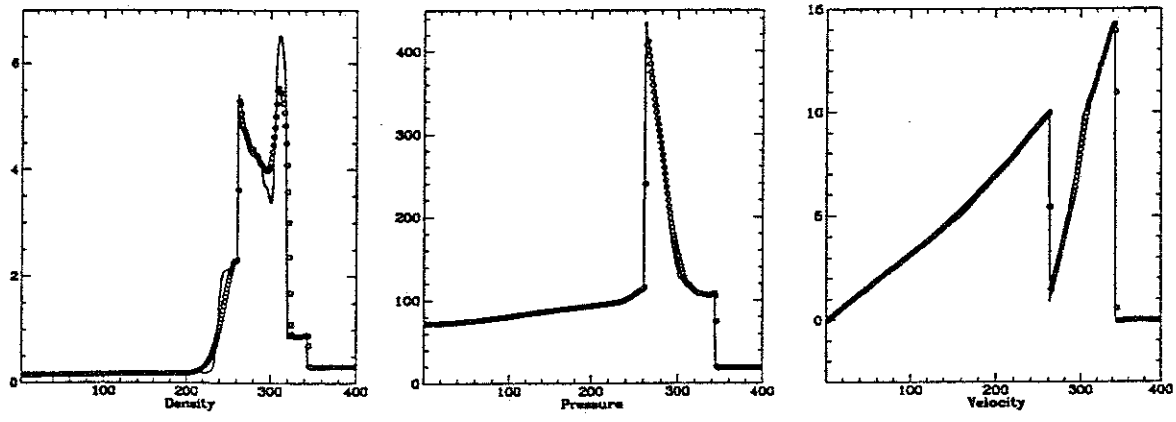

Figure 1.4c : Woodward-Colella test case from 2nd order PTT scheme

flow quantities to make this scheme better. Actually, simple PTT schemes already give very impressive results.

In order to consider the physical collisions between particles more accurately and remedy the excessive dissipation of the beam scheme, the physical collisional models have to be used inside each time step to better describe gas evolution. Ideally, this would require us to solve the full Boltzmann equation, but for many purposes (such as the hydrodynamic limit), some approximate models of the Boltzmann equation are good enough. This thesis is mainly about using an approximate Boltzmann model to develop a new hydrocode.

1.5 Other Approximate Numerical Boltzmann Methods

The numerical methods of solving the original Boltzmann equation or its simplified collisional models are scattered in the literature. In the 1970's, Chorin [7] approximated the collision term by a system of algebraic equations, but the equations were not only numerous, but also very cumbersome. In the following, we give two numerical approaches to the approximate Boltzmann model. Probably the best-known model is the Krook equation or Bhatnagar-Gross-Krook model [2] (BGK model hereafter), which can be written (in the one dimensional case) as

$$f_t + uf_x = \frac{(g-f)}{\tau}, \tag{1.22}$$

where the relaxation time τ is, in simple cases, a function of the local density and temperature. (In the next chapter, we will give a more detailed introduction of the BGK model.)

Method One:

One of the early numerical methods for time-dependent flow problems based on the BGK model was given in the papers of Chu [8] in the 1960's. The main idea is to get $f(x,u,T)$ from the initial gas distribution function $f(x,u,0)$ by solving the

BGK model numerically, where T is the time step. In Chu's method, the Chapman-Enskog expansion technique was used directly in the calculation of the evolution of the function f, with an expansion parameter $\hat{\epsilon} = T/\tau$. In his method, the time step T is chosen to be smaller than the collision time τ in order to validate the Chapman-Enskog expansion. This limitation can also be explained by the numerical stability requirement from the stiff right hand side collision term in the BGK model. In Chu's scheme, both space variable x and particle velocity u are discretized. The scheme uses a standard operator splitting technique of separating transport from collisions. During each time step, first, the particle experiences free molecular transport to the substrips of each time step by

$$f^{(0)}(\hat{x}, \hat{u}, \hat{t}) = F(\hat{x} - \hat{u}t, \hat{u}), \tag{1.23}$$

where $\hat{u}, \hat{x}, \hat{t}$ are dimensionless particle velocity, space and time variables. After getting $f^{(0)}$, the local Maxwellian distribution $g^{(0)}$ is constructed, then the first-order approximation of f due to collisions is given by the following equation,

$$\frac{df^{(1)}}{d\hat{t}} = \frac{(g^{(0)} - f^{(0)})}{\tau^{(0)}}$$

$$f^{(1)}(\hat{x}, \hat{u}, 0) = 0, \tag{1.24}$$

where the second equation $f^{(1)} = 0$ is based on the assumption of Maxwellian distribution for f at the beginning of each time step, and the integration for $f^{(1)}$ is carried out numerically by the trapezoidal rule including the middle levels inside each time step. After solving Eq.(1.24) numerically, the final distribution function f at time T is composed of two terms, which are

$$f(x, u, T) = f^{(0)}(x, u, T) + \hat{\epsilon} f^{(1)}(x, u, T), \tag{1.24}$$

where $f^{(0)}$ is the free advection term (Eq.(1.23) and $f^{(1)}$ is the collision term.

Chu's scheme was first applied to the shock tube problem and shock structure calculations. Lately, it was also used for the simulation of Rayleigh boundary layer problems for rarefied gas flow. Several facts determine some properties in the above scheme.

• The velocity space is discretized, which is similar to the Lattice Gas Boltzmann model, where the validity of description of the continuous gas flow is limited by the number of discrete particle velocities.

• The separation of the BGK model into advection(zero-th order) and collision(first order)terms generate second order errors, which makes the scheme diffusive and computationally expensive.

• The collision time τ is larger than the time step T, which naturally sets the application limit for this scheme to rarefied gas dynamics.

Method Two:

The second numerical approach to the BGK model is a combination of the kinetic equation with an upwinding method (Satofuka *et al* [35] and references therein), which was developed in the 1980's.

The scheme comprises two parts — spatial discretization and time integration. First, the original BGK model is rewritten as

$$f_t = \frac{(g-f)}{\tau} - uf_x. \tag{1.25}$$

In the spatial discretization stage, the spatial derivative in Eq.(1.25) is discretized by second order upwind differencing. For example, the x derivative of f at grid point i is approximated as

$$\frac{\partial f}{\partial x_i} = \begin{cases} -3f_i + 4f_{i+1} - f_{i+2}/2\Delta x, & u > 0 \\ 3f_i - 4f_{i-1} + f_{i-2}/2\Delta x, & u < 0 \end{cases} \tag{1.26}$$

where Δx is the grid spacing size, i is the grid index, and u is the particle velocity. Substitution of the spatial discretization into Eq.(1.25) yields the ordinary differential equation in time,

$$\frac{df}{dt} = G(f). \tag{1.27}$$

Then, the time integration for the above equation can be an implicit Runge-Kutta method, and the largest time step will depend on the detailed integration method, which usually relaxes the requirement $T < \tau$. This method can be naturally extended to higher dimensions by simply adopting operator splitting techniques. Similar to method one, this numerical scheme is diffusive too. As mentioned by Oguchi *et al*[29], the difficulty pertinent to the treatment of the collision term still remains.

Starting in the next chapter, we will present a new numerical treatment of the BGK model, from which we develop highly accurate hydrodynamic schemes for solving the Navier-Stokes and Euler equations.